JCTA Journal of Computing Theories and Applications ISSN:3024-9104

Research Article

Enhanced Diagnosis of Skin Cancer from Dermoscopic Images Using Alignment Optimized Convolutional Neural Networks and Grey Wolf Optimization

Faheem Mazhar [1,*], Naeem Aslam [1†], Ahmad Naeem [1†], Haroon Ahmad [2†], Muhammad Fuzail [1†], and Muhammad Imran [1]

[1] Computer Science Department, NFC Institute of Engineering and Technology, 59030, Multan, Punjab, Pakistan; e-mail : faheemmazharbalouch@gmail.com; naeemaslam@nfciet.edu.pk; ahmad.naeem@nfciet.edu.pk; fuzail@nfciet.edu.pk; muhammad.imran6898@gmail.com
[2] Department of Computer Science, Air University, Islamabad, 44230, Capital, Pakistan; e-mail : haroon@aumc.edu.pk
* Corresponding Author : Faheem Mazhar
† These authors contributed equally to this work.

Abstract: Skin cancer (SC) is a highly serious kind of cancer that, if not addressed swiftly, might result in the patient's demise. Early detection of this condition allows for more effective therapy and prevents disease development. Deep Learning (DL) approaches may be used as an effective and efficient tool for SC detection (SCD). Several DL-based algorithms for automated SCD have been reported. However, more efficient models are needed to improve accuracy. As a result, this paper introduces a new strategy for SCD based on Grey Wolf optimization (GWO) methodologies and CNN. The proposed methodology has four stages: preprocessing, segmentation, feature extraction, and classification. The proposed method utilizes a Convolutional Neural Network (CNN) to extract features from Regions of Interest (ROIs). CNN is employed for feature categorization, whereas the GWO approach enhances accuracy by refining edge detection and segmentation. This technique utilizes a probabilistic model to accelerate the convergence of the GWO algorithm. Employing the GWO model to optimize the structure and weight vectors of CNNs can enhance diagnostic accuracy by a minimum of 5%, based on evaluation outcomes. The application of the proposed strategy and its performance comparison with other methods indicate that the proposed method with GWO predicted SC with an average accuracy of 95.11% and without GWO an Accuracy of 92.66%, respectively, enhancing accuracy by a minimum of 2.5% when we train our model with GWO.

Keywords: CNN; Deep Learning; Grey Wolf Optimization; Skin Cancer; HAM10K.

Received: December, 19th 2024
Revised: January, 7th 2025
Accepted: January, 9th 2025
Published: January, 15th 2025

1. Introduction

The skin, the biggest organ in the body, protects against heat, UV radiation, and infection, yet cancer poses a major threat to human life[1]. Numerous cancer kinds can impact the human body, although one of the most lethal and rapidly proliferating tumors is skin cancer [2]. Statistics from the Skin Cancer Foundation indicate that one in five Americans may develop skin cancer during their lifetime, and one in three cancer diagnoses pertains to skin cancer[3]. Around 3.5 million new cases are annually recorded in the USA, with a continuous increase in incidence[4]. Skin cancer, a significant global health issue, has garnered extensive scientific attention owing to its potential severity and high prevalence. Promptly identifying and accurately classifying skin cancer types is essential for effective treatment[5]. Conventional diagnostic methods, including eye assessments and biopsies, are invasive, labor-intensive, and susceptible to human error. This underscores the necessity for enhanced diagnostic instruments that are both precise and effective[6].

Deep learning (DL) possesses significant potential in this domain. DL is a subset of artificial intelligence that uses algorithms analogous to human cognitive processes to analyze extensive datasets. Numerous cutaneous malignancies originate in the epidermal layers of the

skin. Skin malignancies arise when skin cells proliferate and expand uncontrollably. New epidermal cells frequently develop as old cells perish or sustain injury[7]. When this mechanism fails, cells proliferate rapidly and unevenly. This is why these cells are referred to as tumors, which take the form of a collection of tissue. Factors contributing to this condition include alcohol use, smoking, allergies, infections, environmental changes, and exposure to UV radiation. In addition, abnormal swellings on the body might lead to skin cancer[8]. Skin cancer is classified into seven types: MEL, PGH, MN, DF, BKL, BCC, and AKIEC[9]. Melanoma is the most deadly type of cancer due to its rapid metastasis to other organs. It originates in skin cells known as melanocytes[10]. Melanocytes in the skin produce dark pigments that are typically black and brown but can also be red, purple, and pink. Melanoma cells typically spread to other organs, including the brain, liver, and lungs[11]. Melanoma cancer causes 10,000 fatalities yearly in the United States.

Early detection allows for effective treatment of Melanoma. It is not more prevalent than others. Various types of skin cancer[12]. Pigmented moles known as melanocytotic nevi (MN) can appear in various skin tones. This usually happens in childhood and early adulthood, when the body's moles increase until age thirty to forty[13]. Basal cell (BCC) represents the most prevalent kind of skin cancer. Round cells seen in the lower epidermis frequently exhibit gradual development. Basal cells predominantly impact body areas exposed to sunlight[14]. This type of cutaneous carcinoma seldom metastasizes and is due to uncontrolled cellular proliferation. It may manifest as a diminutive, flesh-toned, or white neoplasm demonstrating bleeding[15]. Squamous cells (SCC) comprise flattened cells in the top epidermis. Cancer cells can emerge when cells grow without regulation. It may present as a solid red lesion or an open wound that hemorrhages profusely. Squamous cell carcinoma (SCC), a kind of skin carcinoma resulting from sun exposure, can manifest in many locations but is frequently non-threatening. It may also manifest on skin that has previously sustained burns or chemical damage[16].

Machine learning approaches, including Support Vector Machine (SVM), Naïve Bayes (NB) [17], and Decision Tree (DT)[18], have been used to classify skin cancer. CNN has surged in prominence in recent years owing to its automated feature extraction capabilities and extensive application in research. Despite rising mortality rates, early detection and intervention can enhance survival probabilities by more than 95% [19]. Our objective is to preserve lives by creating a framework for promptly identifying cutaneous malignancies.

In a study [20], researchers validated a CNN model with around 12,000 publicly available dermoscopic pictures and found that the model outperformed 136 out of 157 physicians in detecting malignant Melanoma. Many deep learning models now produce likelihood ratings for melanoma diagnosis; however, their opaque "black box" nature raises concerns about interpretability, potentially misleading physicians. In response, many researchers have examined CNN models that identify dermoscopic features and replicate the criteria used for melanoma diagnosis, aiming to produce improved diagnostic outcomes through ensemble learning and transfer learning. Furthermore, sophisticated methodologies like generative adversarial networks[21], multitask learning[22], and improved data augmentation have emerged in recent years. CNN models have significantly improved melanoma diagnosis when applied to high-quality standardized dermoscopic images.

2. Related Work

Specialists skilled in multimedia applications and technologies. They underscored that advancing cost-effective identification techniques, such as artificial intelligence, might revolutionize patient testing practices and improve the efficiency of medical care delivery. In recent years, researchers and developers have sought to construct several deep-learning algorithms for detection, segmentation, and classification. A group of researchers conducted pertinent investigations. Nahata and Singh[23] utilized ConvNet to categorize over 35,000 photos from the ISIC dataset in 2018 and 2019. They employ several classification models. Bansal et al. [24] utilized three distinct morphological techniques to improve dermatoscopic pictures. This study included attributes obtained from dermoscopic pictures. The suggested model achieves an accuracy of 94.9% on the HAM10000 dataset and 98.0% on the PH2 dataset.

Shetty et al. [25] advocated data augmentation to improve model accuracy. This work uses K-fold cross-validation to ensure model robustness. The classification accuracy was evaluated using CNN models and machine learning techniques. The research demonstrates that

the suggested CNN exceeds other common methods in terms of accuracy. Kaur et al. [26] presented an automated classifier for Melanoma employing deep CNN. The objective was to improve the detection of melanoma skin cancers by employing a more efficient and simplified deep CNN algorithm relative to existing methods. Omeroglu et al. [27] introduced a network of roadways distinguished by multiple limbs and the hybrid amalgamation of mapping attributes from several modalities. These branches enable the examination of multimodal interactions and the extraction of particular elements. Ding et al. [28] present an innovative approach for melanoma detection. The suggested method entails first data normalization to improve the quality of input images. In the subsequent phase, the Gray-Level-Matrix (GLCM) is employed to ascertain image characteristics. GLCM acquires the texture data for the images. SVM is employed to classify specific attributes and differentiate between benign and malignant tumors. The dataset from the American Cancer Seciety(ACS) is employed to validate the proposed methodology.

The proposed technique outperforms all alternative alternatives in every performance criterion. The proposed method accurately detects Melanoma accompanied by an 88% precision rate. Dahou et al. [29] delineate an advanced skin cancer detection system that utilizes a MobileNetV3 architecture for feature extraction and training to enhance accuracy. The acquired attributes are subsequently input into an enhanced optimization technique called Hunger Games Search (HGS). To ascertain the more pertinent attribute and enhance the model's efficacy, in contrast to 88.19% on the ISIC-2016 dataset. The proposed method surpassed conventional algorithms in feature optimization and classification accuracy for skin cancer detection. Moldovan et al. [30] employed the HAM10000 dataset to introduce a deep learning and transfer learning methodology. The Python-based classification technique categorizes skin cancer images through a two-step PyTorch procedure. The prediction model for the initial step achieved an accuracy of 85.0%, but the model for the subsequent phase attained an accuracy of 75.0%. The constraints of manual methods are addressed through the application of technology in early cancer diagnosis, thereby establishing a novel area of research.

In recent decades, deep learning has revolutionized machine learning. The utilization of artificial neural networks in machine learning is the topic's innovative aspect[31]. CNN is a deep learning model that outperforms traditional techniques in image and feature recognition [32]. This study [33] focuses on developing an ensemble machine-learning model for classifying erythematous-squamous Diseases (ESD). The ensemble approaches integrate five distinct classifiers—NB, SVM, DT, Random Forest (RF), and Gradient Boosting (GB)—by amalgamating their predictions and employing them as input features for a metaclassifier throughout the training process. This paper [34] introduces a sophisticated multi-class skin lesion classification method with an ensemble model that integrates the Inception-V3, ResNet-50, and VGG16 architectures. The classification job aims to categorize skin lesions into certain classifications, such as Melanoma, basal cell carcinoma (BCC), and squamous cell carcinoma (SCC), utilizing the ISIC dataset, which comprises an extensive collection of dermoscopic pictures.

A comparison with alternative approaches is presented in Table 1.

Table 1. Comparison with different Existing Techniques.

Ref	Model	Dataset	Limitations	Accuracy
[24]	HC+DLM	ISIC2018	High computational cost	94.9%
[25]	CNN	HAM10K	Limited training data	95.19%
[35]	DCNN	ISIC 2017	High computational cost	94%
[26]	Deep CNN	ISIC 2016, ISIC2017, ISIC2020	Vulnerable to occlusions	90.42%
[27]	Xception	Seven-point dataset	No local optimization	83.04%

The following exemplifies the research's major contribution:

- GWO is used to optimize CNN's hyperparameters and model a reasonably priced CNN classifier.
- The suggested model is contrasted with a hyper-parameter optimization strategy based on GA and PSO.
- To confirm the efficacy of the suggested approach, extensive experiments are carried out on the HAM 10000 dermoscopic multi-class skin cancer image dataset.

3. Proposed Method

This section evaluates the proposed model's efficacy compared to six recognized deep CNN architectures VGG19, ResNet152, Vgg16, MobileNet, InceptionV3, and Efficient-NetB0.

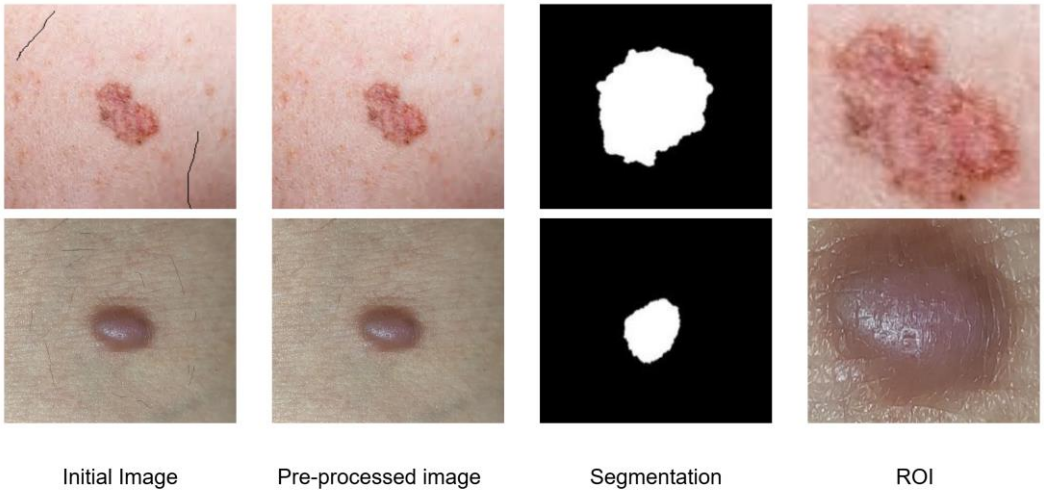

Figure 1. Preprocessing, segmentation, and extraction of regions of interest for specific samples

3.1. Hybrid Model for the Diagnosis of Cutaneous Malignancies

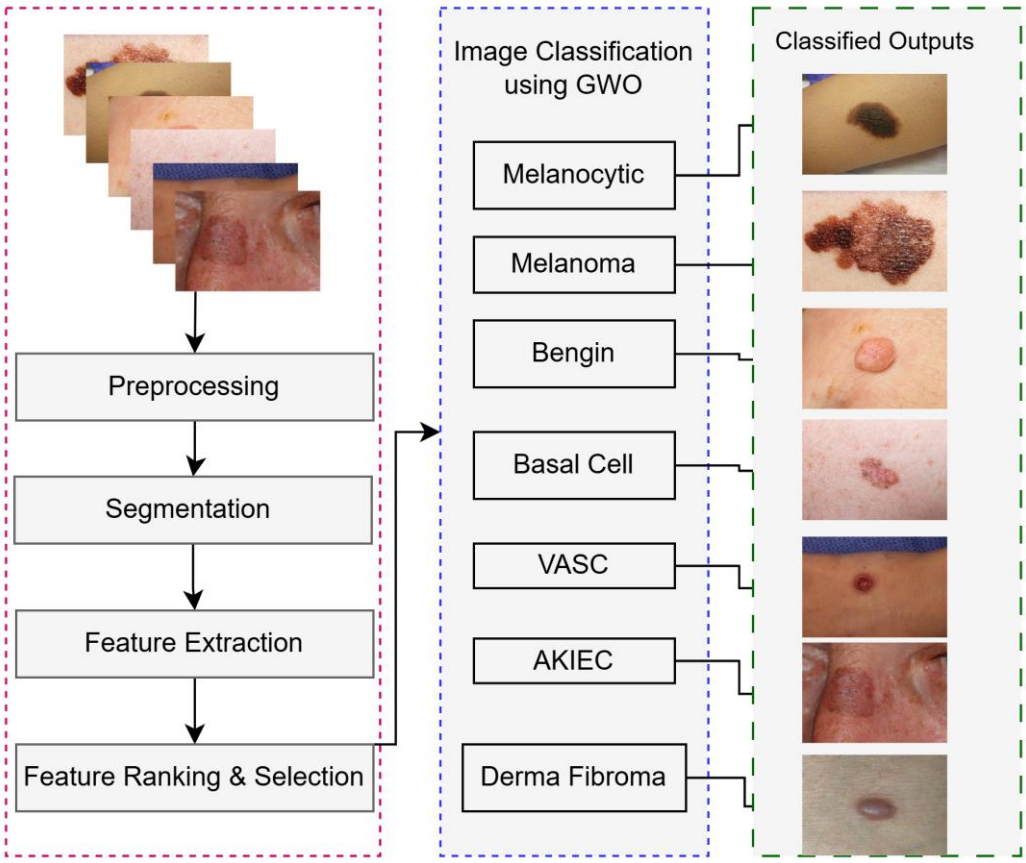

Figure 2. Basic block diagram for identifying skin diseases

UV radiation alters the DNA of skin cells, disrupting their normal development and leading to skin cancer. Researchers commonly use dermoscopic images to detect skin cancer. DL algorithms, including Melanoma (MEL), Basal Cell Carcinoma (BCC), Melanocytic Nevi

(MN), and Squamous Cell Carcinoma (SCC), improve the accuracy of detecting skin malignancies. Early skin cancer detection allows healthcare practitioners to avoid disease progression and initiate treatment sooner. Artificial intelligence and image processing have revolutionized the medical industry. Image processing is widely used in medical analysis[36]–[38]. The research community is essential in advancing intelligent automated systems for precise and prompt assessments and their continual enhancement. We developed a model, an automated method for detecting skin malignancies. The algorithm was trained and assessed using images of seven principal categories of skin cancer Actinic Keratoses and Intraepithelial Carcinomae (AKIEC), Dermatofibroma (DF), Vascular (VASC), Basal Cell Carcinoma (BCC), Benign Keratosis-like Lesions (BKL), Nevus (NV), and Melanoma (MEL) [38]–[40]. The resolution of the provided image is 150 × 150 pixels.

Additionally, the dataset was normalized to avert model overfitting. We employed the (SMOTE) Tomek to rectify the problem of imbalanced dataset distribution and equalize sample sizes across classes[41]. The dataset about cutaneous cancer is categorized into three sets: training, testing, and validation.

Figure 2 illustrates workflow regarding the proposed paradigm for carcinoma of the skin. Relative to [42], the training parameter is diminished. The experimental methodology was executed for a period of up to 30 epochs. At the end of all epochs, the suggested model attained the necessary accuracy in both training and validation. The suggested technique was assessed using six trained classifiers, focusing on accuracy, loss, precision, recall, AUC, and score [43]. The GradeCAM heat-map method has been utilized to depict the visual characteristics of skin cancer that highlight the features influencing its classification. These attributes have been utilized to emphasize factors that aid in detecting skin carcinoma[44].

3.2. Dataset

The dataset consists of skin lesions, which are categorized into seven categories. Dermatoglyphics are preserved using several techniques. The ISIC repository contains 10,015 publicly accessible samples. This study utilized the HAM-10000 dataset, comprising seven categories, to diagnose skin cancer. Figure 2 illustrates a block diagram for the identification of skin cancer.

Table 2. HAM 10000 Dataset.

Dataset	Classes	Training set 85%	Validation set 5%	Test set 10%	Total Images
HAM-10000	7	8513	500.75	1001.5	10,015

3.3. Structure of Proposed Model

The CNN architecture draws inspiration from the biological structure of the human brain, making it particularly adept at computer vision tasks such as object recognition, image segmentation, and facial detection[45]. A CNN's translation or spatial invariance allows it to recognize the same feature in several images, independent of their location[46]. This work created a reliable model using the CNN model to diagnose skin carcinoma conditions properly. The model has five convolutional blocks, a Rectified Linear Unit (ReLu) Activation function, one dropout layer, two dense layers, and a SoftMax classification layer[47].

3.4. Classification using CNN

CNNs are well-liked methods that perform mathematical linear operations using feature vectors [48]. A CNN operates in two phases during training: forward propagation and backward propagation. After multiplying the input and weights, the filter matrix performs a convolutional operation to determine the output [49]. The errors occurring during the forwarding method are assessed using this output. The parameters are changed to account for the final prediction mistakes during the backpropagation process [50]. Identifying errors involves comparing outcomes with ground truth and applying the cost function. To minimize errors, ascertain the gradient of the parameter and adjust accordingly. A CNN excels in classification tasks involving image-based datasets [51]. This study employed CNN to multiclassify skin cancer into eight distinct categories.

3.5. Fundamental Models

This work uses four models to predict skin cancer disease and optimize technique.

3.5.1. EfficientNetB0(B1)

The Efficient Net architecture maximizes model performance by striking a balance between depth, breadth, and resolution. The objective is to achieve an optimal equilibrium between model size and accuracy. EfficientNetB0B1 is utilized when fewer computational resources are necessary. EfficientNetB0B1 is well known for its precise performance, low processing requirements, and sensible number of layers. It is frequently used in computer vision applications such as object detection and image classification[52].

3.5.2. MobileNetV3(B2)

MobileNetV3 is a CNN-based app optimized for mobile devices with limited computational resources. This enhanced iteration of the original MobileNet architecture employs depth-wise separable convolutions, inverted residuals, and linear bottlenecks. Despite low computational resources, it excels in object identification and image classification [53].

3.5.3. DenseNet-169(B3)

DenseNet-169 is a variant of DenseNet, a CNN characterized by dense connections. The network's designation is the numeral "121" to denote the number of layers. DenseNet169 follows a dense connection topology, with each previous layer providing direct input to the next. This connection architecture enhances information transfer across networks by using characteristics. DenseNet-169 is well-known for its effectiveness in training deep neural networks and addressing vanishing gradients[54].

3.5.4. ResNet-101(B4)

One variant of ResNet is called ResNet-101. The"101" in the name indicates the number of network tiers. Residual blocks, which bypass connections and enable the network to acquire residual mappings more effectively, are a hallmark of the ResNet architecture. This architectural design includes a flexible solution to the vanishing gradient problem, which addresses the challenge of training deep neural networks. ResNet-101 is often used in computer vision for several tasks, such as image classification and object identification. It is suitable for many applications due to the trade-off between model depth and computing performance[55].

3.6. Grey-wolf optimization approach

Figure 3 shows the hyperparameter-optimized CNN. The retrieved layers and dimensions are categorized and processed using decision. The choice is susceptible to optimizing attributes and the data set. The CNN architecture ensures the consistency of a feedback-based self-learning environment. Grey wolf optimization (O_G) reduces and provides range characteristics for (TX) and $D(P)\ S0$, resulting in $DP\ S\ =\sim\ TX$ and $(TX\ /\in\ DX)$.

At the initial and final computational phases. The alignment method involves varying parameters in the attribute A_i to achieve $\forall A_i\ \Rightarrow\ DX$ and ($A_i \subseteq DX$) at the outset. The formulation vector is then generated in Equations (1) and (2).

$$[O_G = \lim_{\Delta S \to \infty} \left[\frac{\delta(\Delta Tx)}{\delta t}\right] \otimes \omega(\|D_P\|\iota^0)] \tag{1}$$

$$[\therefore O_G = \lim_{\Delta S \to \infty} \prod_{i=1}^{\eta} \sum_{j=1}^{S} \left(\frac{\delta(\Delta Tx)_{(i,j)}}{\delta t} \otimes \omega\left(\|D_P\|_{\iota^0}^{S}\right)\right)] \tag{2}$$

Where O_G represents an observable quantity, which could signify a measurable quantity or a specific operator being evaluated under certain conditions, such as when $\Delta S \to \infty$. The notation $\lim_{\Delta S \to \infty}$ indicates a limiting process where the entropy (S) approaches infinity, implying a connection to equilibrium states or asymptotic behavior in thermodynamic systems. The component $\omega(\|D_P\|\iota^0)$ likely represents a weighting function ω, applied to the norm of the norm $\|D_P\|$ of a quantity D_P. The superscript ι^0 may indicate either an initial state or a unit vector, depending on the context.

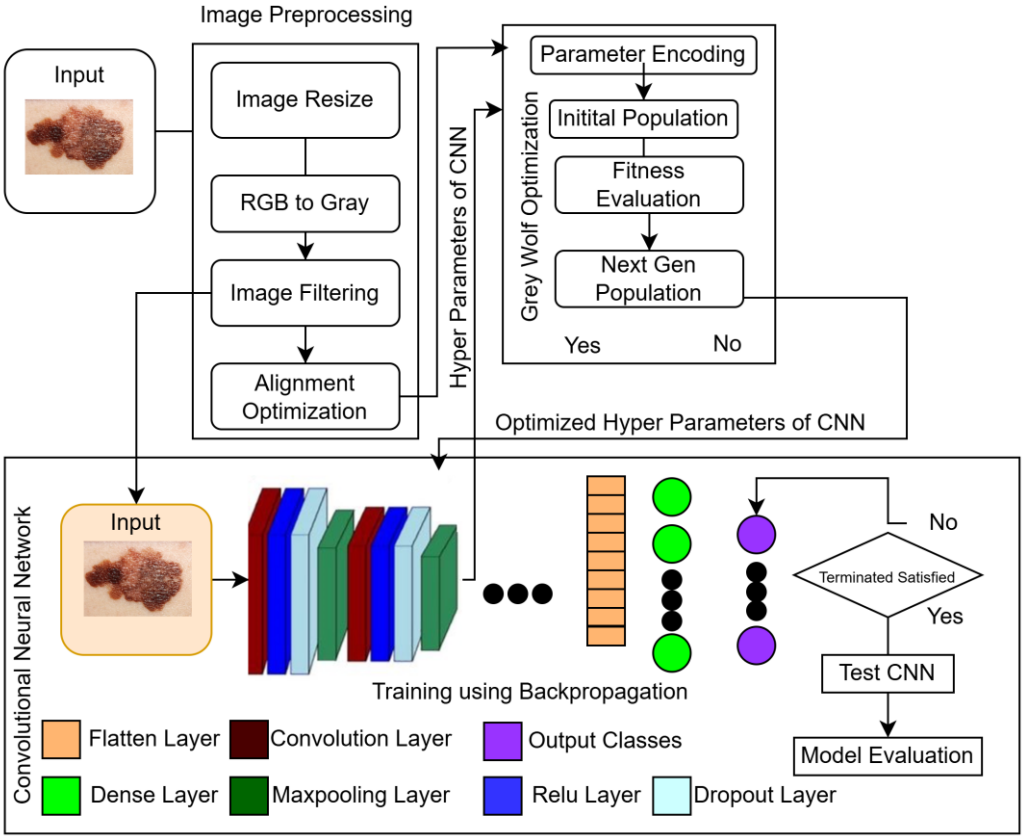

Figure 3. A hyper-parameter-optimized CNN model based on GWO is proposed.

For collective processing, observable quantities (O_G) in the GWO context, is used for the learned neural networking framework. The weight of association corresponds to such that where (x) is the functional variable of optimized approaches. The product term $\prod_{i=1}^{\eta}$ represents the interaction of multiple components or processes indexed i, while the summation $\sum_{j=1}^{S}$ considers the contributions from different states or elements j. The term $\frac{\delta(\Delta Tx)_{(i,j)}}{\delta t}$ represents the time rate of change of the temperature difference (ΔTx) for each component in the system. The tensor product operation $\otimes$ is applied to this rate of change alongside the weighting function $\omega\left(\|D_P\|_{\iota^0}^{S}\right)$, which involves the norm of a quantity D_P and an initial state represented by ι^0 and an additional parameter S.

$$[\mathbb{R}_Y = \lim_{n\to\infty}\left(\mathrm{U}\lim_{n\to S}\left(\frac{\partial^2(O_G)}{\partial t^2}\oplus \Delta T\right)\right)] \tag{3}$$

$$[\therefore \mathbb{R}_Y = \lim_{n\to\infty}\left(\frac{(L\|D_P\|\iota^0)}{L(t)}\prod_{i=1}^{\eta}\sum_{j=1}^{S}\left(\frac{\partial^2(O_G)_j \cap \partial^2(Dx)_k}{\partial t^2}\oplus \Delta T\right)\right)] \tag{4}$$

Where $\mathbb{R}_Y$ is the result of a limit as $n \to \infty$, involving an intersection of operations and second-order derivatives of a function O_G with respect to time $\left(\frac{\partial^2(O_G)}{\partial t^2}\right)$ and spatial terms like (ΔT). L might represent a function of time, and D_P and ι^0 could be associated with some boundary conditions or initial settings. The product $\prod_{i=1}^{\eta}$ and summation $\sum_{j=1}^{S}$ in this equation signify interactions between various terms or variables, with the second derivative terms of O_G interacting with spatial gradient terms such as $(Dx)_k$.

Equations (3) and (4) state that the optimization (O_G) under a constant recurrence format constrains the formulation of datasets. For computational efficiency, a recurrence ratio's functional form is usually evaluated. The dataset's evaluation sequence and occurrence ratio is

subsequently subjected to the removal of inter-common attributes and features, as delineated in Equation (4). The buffer factor guarantees that threshold values are maximized within the dataset's confines. Figure 4 illustrates the skin illness utilizing the proposed GWO Algorithm.

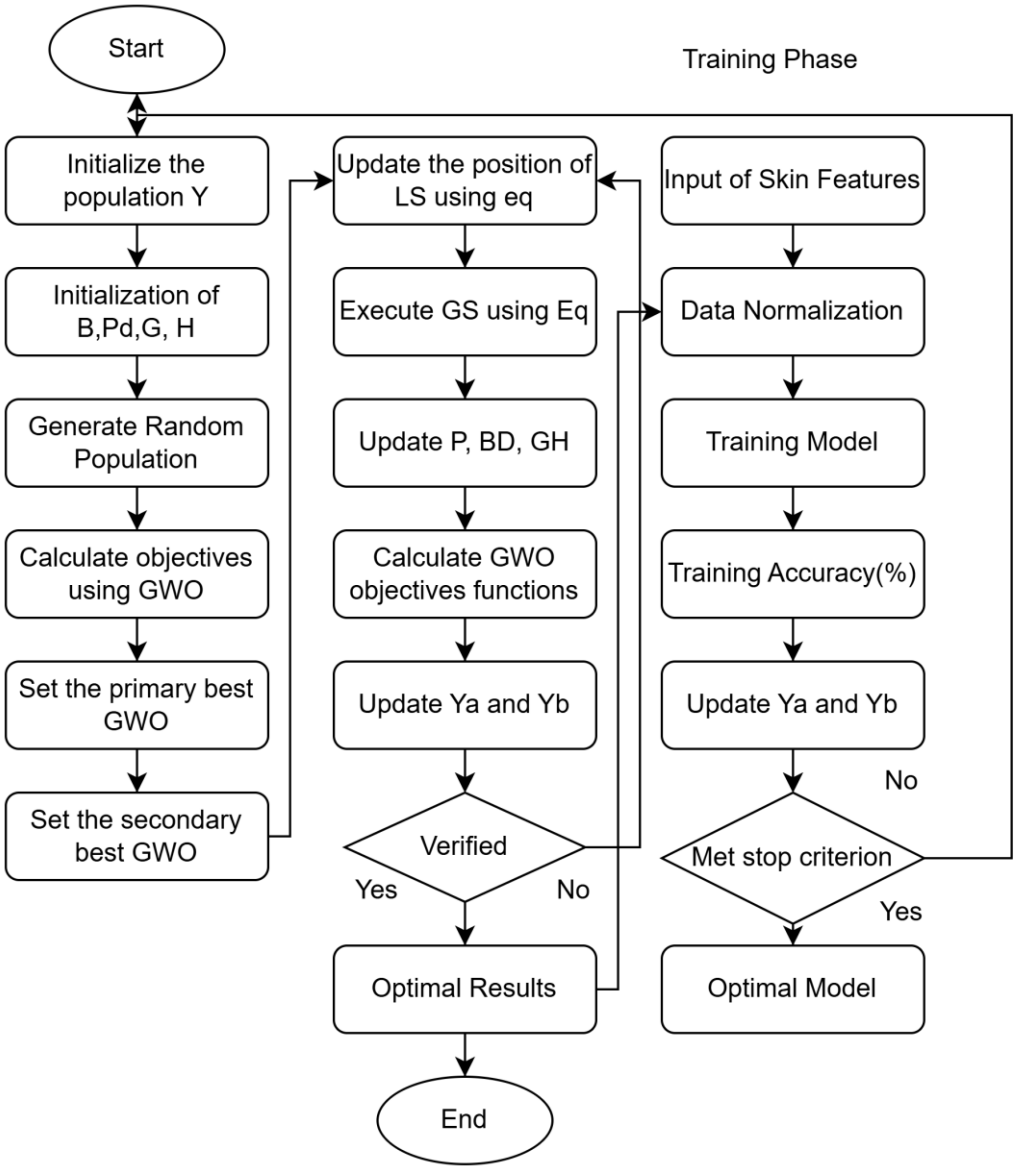

Figure 4. Flow chart for skin disease categorization using the proposed GWO algorithm

4. Results and Discussion

The proposed model is assessed throughout the training and validation phases using several hyperparameters and tuning techniques, including loss function and optimizer metrics. We utilized the ADAM optimizer, a stochastic optimization algorithm. Stochastic optimization methods utilize random minibatches of data to calculate the gradient of the loss function. Early halting is activated. The objective is to avert overfitting by ceasing training when the validation loss escalates. Employing a reduced learning rate to enhance training efficiency through dynamic adjustment. The epoch duration is 50, accompanied by a batch size of 32.

4.1. Model Evaluations

We analyzed dermoscopy images to evaluate the model's ability to classify eight kinds of skin cancer accurately. After training each model, data from each technique stage was utilized to generate confusion matrix-based performance parameters. The Model performance on the testing dataset was evaluated using several measures, such as accuracy (accur), recall (reca) or

sensitivity, f1 score(f1s), precision(prec), true positive (TP), true negative (TN), false positive (FP), and false negative (FN). All measurements were calculated using Equation (5)-(8).

Table 3. Proposed model hyper-parameters.

Parameter	Value
Epochs	50
Optimizer	Adam
Learning rate	0.001
Kernel size	3
Dropout	0.4

$$accur = \frac{TP + TN}{TP + TN + FN + FP} \tag{5}$$

$$prec = \frac{TP}{TP + FP} \tag{6}$$

$$reca = \frac{TP}{TN + FP} \tag{7}$$

$$f1s = \frac{2 \cdot prec \times reca}{prec + reca} \tag{8}$$

The proposed SCD categorizing and verifying approach is backed by flexible datasets, including preprocessed and training data. The technique involved extracting and mapping features from raw datasets using schematic records regarding the trained dataset repository. Figure 5 illustrates the method of extracting attribute ratios over several situations. A feature matrix with interconnected values is produced by linking the alignment ratios of separate attributes. This includes the alignment ratio-based feature selection performance efficiency of attribute ratios for a specific range of values. The division ratio between the training and testing datasets dictates the scenario.

Figure 5. Extracting attribute ratios and comparing assessment parameters

4.2. Discussion

Figure 6 compares the performance of the proposed GWO strategy to known approaches, including feature and KNN optimization and whale optimization. The suggested GWO-based feature optimization achieved 95.82% accuracy, outperforming competing

approaches. The proposed Trained Convolutional Neural Networking (CNN) architecture is assessed using Recursive Learning (RL) based on extracted values from numerous comparisons (see Fig. 7). CNN+RL-based computation improves decision-making and assistance. The RL extends the CNN model's feedback layer by incorporating structural modifications to processing (hidden layers). A minimum navies strategy optimizes the prediction and classification ratio by limiting the ratio of TNR to FPR. Various cross-domain techniques, such as KNN, whale optimization, and GWO, are employed to evaluate and validate anticipated results. Independent data processing and decision-making abilities are necessary for this approach. Performance ranges from KNN to whale optimization, depending on the situation. These optimization techniques are system-driven as they place a high priority on centralization and dataset preservation. Network CNN+RL models in FSs are the focus of GWO. The decentralized structure of the federated learning framework makes it more computationally efficient than alternative methods. The federated learning (FL) and Recursive Learning (RL) models of CNN are used to investigate the GWO process using interdomain computation.

Table 4. Evaluating the effectiveness of the proposed model in comparison to other approaches.

Method	Dataset	MCC	CSI	Accur	Reca	F1S	Prec
ANN+ IGWO [56]	ISIC 2016	0.9131	0.8636	97.0976	95.5817	97.1864	94.1755
CNN Only [57]	-	0.7967	0.6867	92.8760	89.5416	92.546	87.2953
ANN (LM) [58]	-	0.8029	0.6953	93.1398	89.8846	92.7105	87.7296
ANN+GWO [59]	-	0.8830	0.8171	96.0422	94.0309	96.0263	92.3487
ANN+ IGWO [60]	ISIC 2017	0.8641	0.7928	95.1667	92.8606	96.3503	90.2746
CNN Only [61]	-	0.7767	0.6528	92.3333	88.5792	91.3521	86.4683
ANN (LM)[62]	-	0.7910	0.6783	92.6667	89.1980	92.5307	86.7776
Proposed	HAM10K	0.9155	0.8645	95.1122	94.5612	93.8874	96.1665

*MCC: Matthew's Correlation Coefficient; CSI: Critical Success Index.

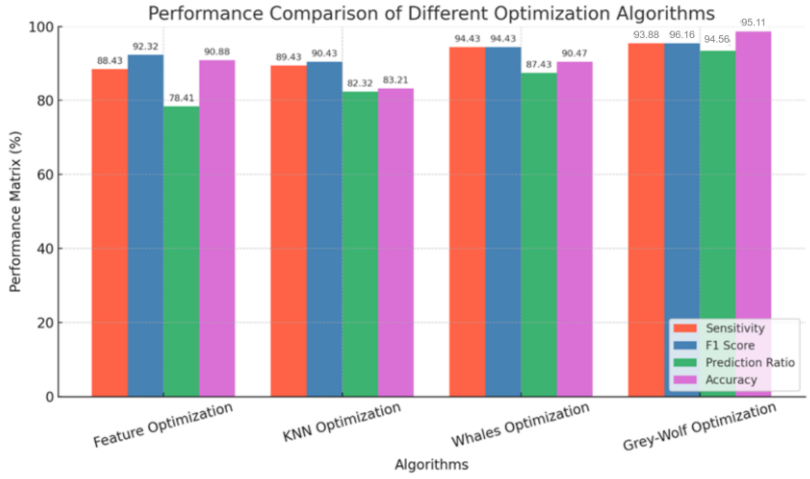

Figure 6. Comparison of proposed method performance with different optimization algorithms

The technique described here has some possible drawbacks that should be considered. Specific optimization techniques such as KNN, Whale, and GWO may limit the generalizability of outcomes since they may not apply to all the available datasets or problem areas. Furthermore, KNN and whale optimization rely on centralized datasets, which may be troublesome for applications with dispersed or privacy-sensitive data. GWO is intricate, particularly when utilized in CNN-based recursive learning models. Multidisciplinary Federated systems may face implementation difficulties. that diminish their efficacy. The computational requirements of the federated learning system, in conjunction with Grey-wolf optimization,

may incur substantial computational expenses. Interdomain computing utilizing FL and Recurrent Studying models of Temporal Neural Networks to enhance GWO may encounter constraints stemming from data heterogeneity and communication expenses. Performance comparisons of optimization approaches may not apply to all datasets or circumstances, thus, it's important to consider dataset features and scalability considerations.

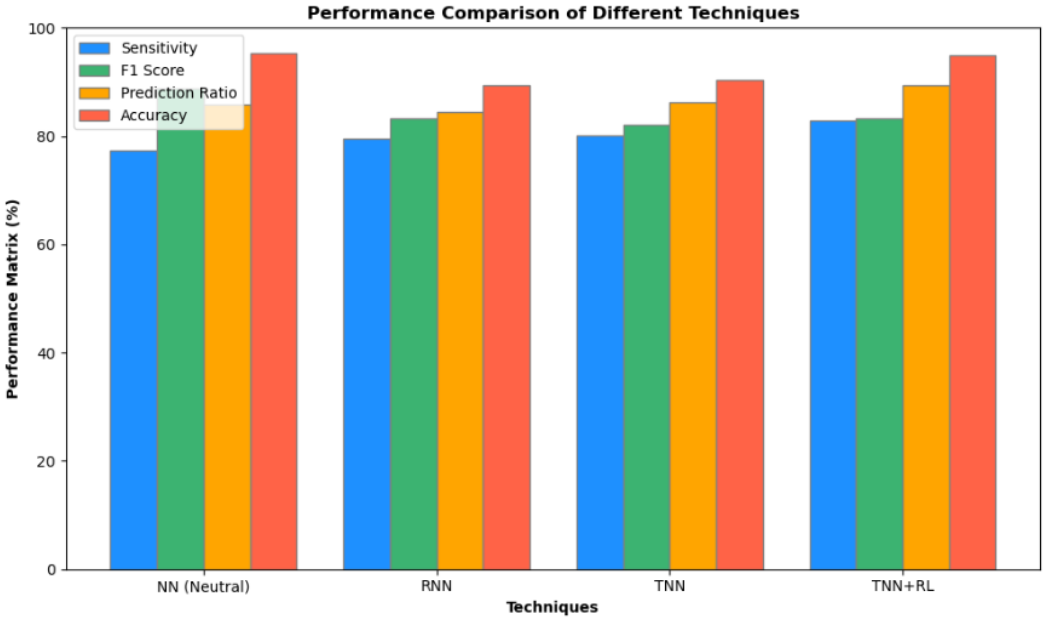

Figure 7. Study evaluation and observation using a trained convolutional neural network technique

Table 5. The suggested model's performance in comparison to baseline techniques

Classifiers	Accur (%)	Prec (%)	Reca (%)	F1S (%)	AUC (%)
VGG16	91.22	93.11	90.52	93.43	94.87
EfficientNetB0	90.23	91.36	89.36	90.85	95.63
MobileNetV3	91.54	90.27	92.78	88.54	93.99
DenseNet-169	90.62	91.51	87.36	90.31	94.44
ResNet-101	91.20	92.33	92.56	93.88	95.33
Proposed Model (With GWO)	95.11	94.56	93.88	96.16	97.65
Proposed Model (Without GWO)	92.66	92.32	91.35	94.36	95.40

*AUC: Area under Curve.

We used the same dataset and GWO to compare our recommended deep neural networks against current ones, including VGG19, ResNet152, EfficientNetB0, Vgg16, InceptionV3, and MobileNetv3. We also compared the planned model before doing the Grey Wolf Optimisation. The system with GWO yields excellent results for the suggested model. Table 5 shows that the proposed models with and without GWO, VGG16, ResNet101, MobileNetv3, EfficientNetB0, and DenseNet-169 achieved accuracies of 95.11%, 92.66%, 91.22%, 91.20%, 91.54%, 90.23%, and 90.62%, respectively.

Alignment optimization is a more successful method than feature and attribute optimization for identifying skin cancer with CNNs, since it adopts a holistic perspective of the entire process. Rather than concentrating exclusively on enhancing input data, it improves each phase—from data preparation and CNN design to hyperparameter fine-tuning and outcome interpretation. This comprehensive viewpoint enables the model to discern intricate patterns and adjust to varied datasets, crucial for dependable medical diagnosis. Optimization of features and attributes, although beneficial, may constrain the model's adaptability and capacity to generalize to novel or diverse scenarios. Integrating alignment optimization with GWO enables simultaneous refinement of many system components, resulting in a more

resilient, precise, and versatile model. This comprehensive strategy is more adept at addressing the practical issues of medical imaging, including variability and complexity, resulting in more dependable clinical outcomes.

Table 6. Comparison of the suggested methodology to SOTA approaches using the HAM10000 dataset.

Model	Accuracy (%)	Precision (%)	Recall (%)	F1- Score (%)
CNN [63]	91.44	96.57	93.56	95.31
AlexNet [64]	85.00	82.20	89.0	87.02
CNN-ResNet [18]	92.95	91.32	91.99	90.21
DenseNet121 [65]	91.05	83.76	95.37	86.44
CNN-ResNet-50 [66]	88.33	77.99	85.83	81.60
MobileNetV2[67]	89.22	78.69	79.49	80.02
Proposed	95.11	94.56	93.88	96.16

Table 6 illustrates the performance of many models, including the proposed approach, on the HAM10000 skin lesion categorization dataset. Critical criteria, including accuracy, specificity, sensitivity, and F1-score, were employed to evaluate the models. The suggested model surpasses current state-of-the-art methods, attaining remarkable results across all metrics: 95.11% accuracy, 94.56% precision, 93.88% recall, and 96.16% F1-score. This significant enhancement can likely be attributed to advancements in feature extraction techniques, improved classification algorithms, or the incorporation of ensemble approaches.

5. Conclusions

This paper presents an effective GWO and skin disease classification strategy for accurately identifying skin diseases. Seven different types of skin disorders were investigated experimentally using HAM-10000 datasets. Each dataset is utilized with separate testing and training samples. For each dataset, performance is measured in terms of sensitivity, accuracy, specificity, precision, recall, F1 Score, and AUC similarity index, and the best results are achieved. The suggested segmentation results are 0.928 in accuracy, 0.946 in specificity, 0.917 in sensitivity, 0.933. In comparison to cutting-edge approaches, the suggested GWO achieves accurate classification results with 95.11% accuracy, 96.16% F1-Score, 97.65% AUC, 93.88% recall, and 94.56% precision.

Future studies seek to improve the suggested GWO-based skin disease classification technique by adapting it for real-time diagnostic systems in clinical settings, assuring speed and reliability. To increase its adaptability, the method may be evaluated on various large-scale datasets and developed to detect a wider spectrum of skin problems, including uncommon illnesses. Combining GWO with additional optimization techniques or deep learning models may increase its accuracy even more, while explainable AI (XAI) might make the system's predictions more transparent and trustworthy to healthcare practitioners. Integrating other diagnostic tools, such as dermoscopic images or clinical data, might boost its usefulness while adapting the system for mobile or cloud platforms, making it more accessible in rural or resource-constrained places. Addressing issues such as class imbalance and implementing advanced data augmentation techniques may also increase its dependability across all skin conditions.

Author Contributions: Conceptualization, F.M. N.A.; methodology, F.M. N.A. and A.N.; software, H.A., and M.F.; validation, F.M. N.A. and A.N.; formal analysis, A.N., and H.A.; investigation, M.I.; resources, M.I. and M.F; data curation, A.N. and H.A.; writing – original draft preparation, F.M.; writing – review and editing, M.F. and A.N. funding acquisition, N.A. All authors have read and agreed to the published version of the manuscript.

Funding: No specific funding was received for this research study.

Data Availability Statement: All data supporting this study are openly available within the paper and online [68] as open source, without restrictions.

Acknowledgments: All relevant data is within the manuscript and supporting information files.

Conflicts of Interest: The authors have declared that no competing interests exist.

References

[1] M. Sajid, A. H. Khan, T. S. Malik, A. Bilal, Z. Ahmad, and R. Sarwar, "Enhancing Melanoma Diagnostic: Harnessing the Synergy of AI and CNNs for Groundbreaking Advances in Early Melanoma Detection and Treatment Strategies," *Int. J. Imaging Syst. Technol.*, vol. 35, no. 1, Jan. 2025, doi: 10.1002/ima.70016.

[2] F. Piccialli, V. Di Somma, F. Giampaolo, S. Cuomo, and G. Fortino, "A survey on deep learning in medicine: Why, how and when?," *Inf. Fusion*, vol. 66, pp. 111–137, 2021.

[3] N. Razmjooy *et al.*, "Computer-aided Diagnosis of Skin Cancer: A Review," *Curr. Med. Imaging Former. Curr. Med. Imaging Rev.*, vol. 16, no. 7, pp. 781–793, Sep. 2020, doi: 10.2174/1573405616666200129095242.

[4] A. Esteva *et al.*, "Dermatologist-level classification of skin cancer with deep neural networks," *Nature*, vol. 542, no. 7639, pp. 115–118, Feb. 2017, doi: 10.1038/nature21056.

[5] D. E. O'Sullivan, D. R. Brenner, P. A. Demers, P. J. Villeneuve, C. M. Friedenreich, and W. D. King, "Indoor tanning and skin cancer in Canada: A meta-analysis and attributable burden estimation," *Cancer Epidemiol.*, vol. 59, pp. 1–7, Apr. 2019, doi: 10.1016/j.canep.2019.01.004.

[6] E. Chatzilakou, Y. Hu, N. Jiang, and A. K. Yetisen, "Biosensors for melanoma skin cancer diagnostics," *Biosens. Bioelectron.*, vol. 250, p. 116045, Apr. 2024, doi: 10.1016/j.bios.2024.116045.

[7] N. Nordmann, M. Hubbard, T. Nordmann, P. W. Sperduto, H. B. Clark, and M. A. Hunt, "Effect of Gamma Knife Radiosurgery and Programmed Cell Death 1 Receptor Antagonists on Metastatic Melanoma," *Cureus*, vol. 9, no. 12, Dec. 2017, doi: 10.7759/cureus.1943.

[8] A. Naeem, T. Anees, R. A. Naqvi, and W.-K. Loh, "A Comprehensive Analysis of Recent Deep and Federated-Learning-Based Methodologies for Brain Tumor Diagnosis," *J. Pers. Med.*, vol. 12, no. 2, p. 275, Feb. 2022, doi: 10.3390/jpm12020275.

[9] H. W. Rogers, M. A. Weinstock, S. R. Feldman, and B. M. Coldiron, "Incidence Estimate of Nonmelanoma Skin Cancer (Keratinocyte Carcinomas) in the US Population, 2012," *JAMA Dermatology*, vol. 151, no. 10, p. 1081, Oct. 2015, doi: 10.1001/jamadermatol.2015.1187.

[10] L. Bomm, M. D. V. Benez, J. M. P. Maceira, I. C. B. Succi, and M. de F. G. Scotelaro, "Biopsy guided by dermoscopy in cutaneous pigmented lesion - Case report," *An. Bras. Dermatol.*, vol. 88, no. 1, pp. 125–127, Feb. 2013, doi: 10.1590/S0365-05962013000100020.

[11] J. Kato, K. Horimoto, S. Sato, T. Minowa, and H. Uhara, "Dermoscopy of Melanoma and Non-melanoma Skin Cancers," *Front. Med.*, vol. 6, p. 180, Aug. 2019, doi: 10.3389/fmed.2019.00180.

[12] H. A. Haenssle *et al.*, "Man against machine: diagnostic performance of a deep learning convolutional neural network for dermoscopic melanoma recognition in comparison to 58 dermatologists," *Ann. Oncol.*, vol. 29, no. 8, pp. 1836–1842, Aug. 2018, doi: 10.1093/annonc/mdy166.

[13] H. Ibrahim, M. El-Taieb, A. Ahmed, R. Hamada, and E. Nada, "Dermoscopy versus skin biopsy in diagnosis of suspicious skin lesions," *Al-Azhar Assiut Med. J.*, vol. 15, no. 4, p. 203, 2017, doi: 10.4103/AZMJ.AZMJ_67_17.

[14] K. Duggani and M. K. Nath, "A Technical Review Report on Deep Learning Approach for Skin Cancer Detection and Segmentation," in *Data Analytics and Management: Proceedings of ICDAM*, Springer, 2021, pp. 87–99. doi: 10.1007/978-981-15-8335-3_9.

[15] P. Carli *et al.*, "Pattern analysis, not simplified algorithms, is the most reliable method for teaching dermoscopy for melanoma diagnosis to residents in dermatology," *Br. J. Dermatol.*, vol. 148, no. 5, pp. 981–984, May 2003, doi: 10.1046/j.1365-2133.2003.05023.x.

[16] C. Carrera *et al.*, "Validity and Reliability of Dermoscopic Criteria Used to Differentiate Nevi From Melanoma," *JAMA Dermatology*, vol. 152, no. 7, p. 798, Jul. 2016, doi: 10.1001/jamadermatol.2016.0624.

[17] S. Lu, Z. Lu, and Y.-D. Zhang, "Pathological brain detection based on AlexNet and transfer learning," *J. Comput. Sci.*, vol. 30, pp. 41–47, Jan. 2019, doi: 10.1016/j.jocs.2018.11.008.

[18] K. Polat and K. Onur Koc, "Detection of Skin Diseases from Dermoscopy Image Using the combination of Convolutional Neural Network and One-versus-All," *J. Artif. Intell. Syst.*, vol. 2, no. 1, pp. 80–97, 2020, doi: 10.33969/AIS.2020.21006.

[19] M. Z. Alom, T. Aspiras, T. M. Taha, and V. K. Asari, "Skin cancer segmentation and classification with improved deep convolutional neural network," in *Medical Imaging 2020: Imaging Informatics for Healthcare, Research, and Applications*, Mar. 2020, vol. 11318, p. 36. doi: 10.1117/12.2550146.

[20] T. J. Brinker *et al.*, "Deep neural networks are superior to dermatologists in melanoma image classification," *Eur. J. Cancer*, vol. 119, pp. 11–17, Sep. 2019, doi: 10.1016/j.ejca.2019.05.023.

[21] I. Abunadi, "Deep and hybrid learning of MRI diagnosis for early detection of the progression stages in Alzheimer's disease," *Conn. Sci.*, vol. 34, no. 1, pp. 2395–2430, Dec. 2022, doi: 10.1080/09540091.2022.2123450.

[22] J. Kawahara, S. Daneshvar, G. Argenziano, and G. Hamarneh, "Seven-Point Checklist and Skin Lesion Classification Using Multitask Multimodal Neural Nets," *IEEE J. Biomed. Heal. Informatics*, vol. 23, no. 2, pp. 538–546, Mar. 2019, doi: 10.1109/JBHI.2018.2824327.

[23] H. Nahata and S. P. Singh, "Deep Learning Solutions for Skin Cancer Detection and Diagnosis," in *Machine learning with health care perspective: machine learning and healthcare*, Springer, 2020, pp. 159–182. doi: 10.1007/978-3-030-40850-3_8.

[24] P. Bansal, R. Garg, and P. Soni, "Detection of melanoma in dermoscopic images by integrating features extracted using handcrafted and deep learning models," *Comput. Ind. Eng.*, vol. 168, p. 108060, Jun. 2022, doi: 10.1016/j.cie.2022.108060.

[25] B. Shetty, R. Fernandes, A. P. Rodrigues, R. Chengoden, S. Bhattacharya, and K. Lakshmanna, "Skin lesion classification of dermoscopic images using machine learning and convolutional neural network," *Sci. Rep.*, vol. 12, no. 1, p. 18134, Oct. 2022, doi: 10.1038/s41598-022-22644-9.
[26] R. Kaur, H. Gholamhosseini, and R. Sinha, "Melanoma Classification Using a Novel Deep Convolutional Neural Network with Dermoscopic Images," pp. 1–15, 2022.
[27] A. N. Omeroglu, H. M. A. Mohammed, E. A. Oral, and S. Aydin, "A novel soft attention-based multi-modal deep learning framework for multi-label skin lesion classification," *Eng. Appl. Artif. Intell.*, vol. 120, p. 105897, Apr. 2023, doi: 10.1016/j.engappai.2023.105897.
[28] H. Ding, Q. Huang, and A. Alkhayyat, "A computer aided system for skin cancer detection based on Developed version of the Archimedes Optimization algorithm," *Biomed. Signal Process. Control*, vol. 90, p. 105870, Apr. 2024, doi: 10.1016/j.bspc.2023.105870.
[29] A. Dahou, A. O. Aseeri, A. Mabrouk, R. A. Ibrahim, M. A. Al-Betar, and M. A. Elaziz, "Optimal Skin Cancer Detection Model Using Transfer Learning and Dynamic-Opposite Hunger Games Search," *Diagnostics*, vol. 13, no. 9, p. 1579, Apr. 2023, doi: 10.3390/diagnostics13091579.
[30] D. Moldovan, "Transfer Learning Based Method for Two-Step Skin Cancer Images Classification," in *2019 E-Health and Bioengineering Conference (EHB)*, Nov. 2019, pp. 1–4. doi: 10.1109/EHB47216.2019.8970067.
[31] T. Mendonça *et al.*, "PH 2-A dermoscopic image database for research and benchmarking," in *2013 35th annual international conference of the IEEE engineering in medicine and biology society (EMBC)*, 2013, pp. 5437–5440. doi: 10.1109/EMBC.2013.6610779.
[32] S. Keele, others, B. Kitchenham, S. M. Charters, and S. Keele, "Guidelines for performing systematic literature reviews in software engineering," 2007.
[33] O. Jaiyeoba, E. Ogbuju, O. T. Yomi, and F. Oladipo, "Development of a model to classify skin diseases using stacking ensemble machine learning techniques," *J. Comput. Theor. Appl.*, vol. 2, no. 1, pp. 22–38, May 2024, doi: 10.62411/jcta.10488.
[34] K. P. Zaw and A. Mon, "Enhanced Multi-Class Skin Lesion Classification of Dermoscopic Images Using an Ensemble of Deep Learning Models," *J. Comput. Theor. Appl.*, vol. 2, no. 2, pp. 256–267, Nov. 2024, doi: 10.62411/jcta.11530.
[35] E. H. Houssein, D. A. Abdelkareem, G. Hu, M. A. Hameed, I. A. Ibrahim, and M. Younan, "An effective multiclass skin cancer classification approach based on deep convolutional neural network," *Cluster Comput.*, vol. 27, no. 9, pp. 12799–12819, Dec. 2024, doi: 10.1007/s10586-024-04540-1.
[36] J. Yogapriya, V. Chandran, M. G. Sumithra, P. Anitha, P. Jenopaul, and C. Suresh Gnana Dhas, "Gastrointestinal Tract Disease Classification from Wireless Endoscopy Images Using Pretrained Deep Learning Model," *Comput. Math. Methods Med.*, vol. 2021, no. 1, pp. 1–12, Sep. 2021, doi: 10.1155/2021/5940433.
[37] L. Alzubaidi *et al.*, "Towards a Better Understanding of Transfer Learning for Medical Imaging: A Case Study," *Appl. Sci.*, vol. 10, no. 13, p. 4523, Jun. 2020, doi: 10.3390/app10134523.
[38] Y. Yuan, B. Li, and M. Q.-H. Meng, "Bleeding Frame and Region Detection in the Wireless Capsule Endoscopy Video," *IEEE J. Biomed. Heal. Informatics*, vol. 20, no. 2, pp. 624–630, Mar. 2016, doi: 10.1109/JBHI.2015.2399502.
[39] N. Shamsudhin *et al.*, "Magnetically guided capsule endoscopy," *Med. Phys.*, vol. 44, no. 8, pp. e91--e111, Aug. 2017, doi: 10.1002/mp.12299.
[40] B. J. Stewart, J. R. Ferdinand, and M. R. Clatworthy, "Using single-cell technologies to map the human immune system — implications for nephrology," *Nat. Rev. Nephrol.*, vol. 16, no. 2, pp. 112–128, Feb. 2020, doi: 10.1038/s41581-019-0227-3.
[41] H. Han, W.-Y. Wang, and B.-H. Mao, "Borderline-SMOTE: A New Over-Sampling Method in Imbalanced Data Sets Learning," in *International conference on intelligent computing*, 2005, pp. 878–887. doi: 10.1007/11538059_91.
[42] V. Charisis, A. Tsiligiri, L. J. Hadjileontiadis, C. N. Liatsos, C. C. Mavrogiannis, and G. D. Sergiadis, "Ulcer Detection in Wireless Capsule Endoscopy Images Using Bidimensional Nonlinear Analysis," in *XII Mediterranean Conference on Medical and Biological Engineering and Computing 2010: May 27--30, 2010 Chalkidiki, Greece*, 2010, pp. 236–239. doi: 10.1007/978-3-642-13039-7_59.
[43] M. Abra Ayidzoe, Y. Yu, P. K. Mensah, J. Cai, K. Adu, and Y. Tang, "Gabor capsule network with preprocessing blocks for the recognition of complex images," *Mach. Vis. Appl.*, vol. 32, no. 4, p. 91, Jul. 2021, doi: 10.1007/s00138-021-01221-6.
[44] S. Mohapatra, J. Nayak, M. Mishra, G. K. Pati, B. Naik, and T. Swarnkar, "Wavelet Transform and Deep Convolutional Neural Network-Based Smart Healthcare System for Gastrointestinal Disease Detection," *Interdiscip. Sci. Comput. Life Sci.*, vol. 13, no. 2, pp. 212–228, Jun. 2021, doi: 10.1007/s12539-021-00417-8.
[45] S. Wang, Y. Xing, L. Zhang, H. Gao, and H. Zhang, "Deep Convolutional Neural Network for Ulcer Recognition in Wireless Capsule Endoscopy: Experimental Feasibility and Optimization," *Comput. Math. Methods Med.*, vol. 2019, no. 1, pp. 1–14, Sep. 2019, doi: 10.1155/2019/7546215.
[46] T. Yoshitake *et al.*, "Rapid histopathological imaging of skin and breast cancer surgical specimens using immersion microscopy with ultraviolet surface excitation," *Sci. Rep.*, vol. 8, no. 1, p. 4476, Mar. 2018, doi: 10.1038/s41598-018-22264-2.
[47] F. Wen and A. K. David, "A genetic algorithm based method for bidding strategy coordination in energy and spinning reserve markets," *Artif. Intell. Eng.*, vol. 15, no. 1, pp. 71–79, Jan. 2001, doi: 10.1016/S0954-1810(01)00002-4.
[48] H. Malik, M. S. Farooq, A. Khelifi, A. Abid, J. Nasir Qureshi, and M. Hussain, "A Comparison of Transfer Learning Performance Versus Health Experts in Disease Diagnosis From Medical Imaging," *IEEE Access*, vol. 8, pp. 139367–139386, 2020, doi: 10.1109/ACCESS.2020.3004766.
[49] O. Jaiyeoba, O. Jaiyeoba, E. Ogbuju, and F. Oladipo, "AI-Based Detection Techniques for Skin Diseases: A Review of Recent Methods, Datasets, Metrics, and Challenges," *J. Futur. Artif. Intell. Technol.*, vol. 1, no. 3, pp. 318–336, Dec. 2024, doi: 10.62411/faith.3048-3719-46.
[50] K. Thurnhofer-Hemsi and E. Domínguez, "A Convolutional Neural Network Framework for Accurate Skin Cancer Detection," *Neural Process. Lett.*, vol. 53, no. 5, pp. 3073–3093, Oct. 2021, doi: 10.1007/s11063-020-10364-y.
[51] J. Höhn *et al.*, "Combining CNN-based histologic whole slide image analysis and patient data to improve skin cancer classification," *Eur. J. Cancer*, vol. 149, pp. 94–101, May 2021, doi: 10.1016/j.ejca.2021.02.032.

[52] V. Anand, S. Gupta, D. Koundal, S. R. Nayak, J. Shafi, and A. K. Bhoi, "Segmentation and Classification of Skin Cancer Using K-means Clustering and EfficientNetB0 Model," in *Advances in Communication, Devices and Networking: Proceedings of ICCDN 2021*, Springer, 2023, pp. 471–481. doi: 10.1007/978-981-19-2004-2_42.

[53] M. Toğaçar, Z. Cömert, and B. Ergen, "Intelligent skin cancer detection applying autoencoder, MobileNetV2 and spiking neural networks," *Chaos, Solitons & Fractals*, vol. 144, p. 110714, Mar. 2021, doi: 10.1016/j.chaos.2021.110714.

[54] S. Jain and K. Agrawal, "An Efficient Diagnosis of Melanoma Skin Disease Using DenseNet-121," in *2023 3rd International Conference on Technological Advancements in Computational Sciences (ICTACS)*, Nov. 2023, pp. 908–912. doi: 10.1109/ICTACS59847.2023.10390147.

[55] A. Demir, F. Yilmaz, and O. Kose, "Early detection of skin cancer using deep learning architectures: resnet-101 and inception-v3," in *2019 Medical Technologies Congress (TIPTEKNO)*, Oct. 2019, pp. 1–4. doi: 10.1109/TIPTEKNO47231.2019.8972045.

[56] W. Lai, M. Kuang, X. Wang, P. Ghafariasl, M. H. Sabzalian, and S. Lee, "Skin cancer diagnosis (SCD) using Artificial Neural Network (ANN) and Improved Gray Wolf Optimization (IGWO)," *Sci. Rep.*, vol. 13, no. 1, p. 19377, Nov. 2023, doi: 10.1038/s41598-023-45039-w.

[57] M. S. Sivakumar, L. M. Leo, T. Gurumekala, V. Sindhu, and A. S. Priyadharshini, "Deep learning in skin lesion analysis for malignant melanoma cancer identification," *Multimed. Tools Appl.*, vol. 83, no. 6, pp. 17833–17853, Jul. 2023, doi: 10.1007/s11042-023-16273-1.

[58] M. Goyal, T. Knackstedt, S. Yan, and S. Hassanpour, "Artificial intelligence-based image classification methods for diagnosis of skin cancer: Challenges and opportunities," *Comput. Biol. Med.*, vol. 127, p. 104065, Dec. 2020, doi: 10.1016/j.compbiomed.2020.104065.

[59] Z. Xu, X. Zhang, and L. Liu, "M-Net: A Skin Cancer Classification With Improved Convolutional Neural Network Based on the Enhanced Gray Wolf Optimization Algorithm," *Int. J. Imaging Syst. Technol.*, vol. 34, no. 6, p. e23202, Nov. 2024, doi: 10.1002/ima.23202.

[60] R. Mousa, S. Chamani, M. Morsali, M. Kazzazi, P. Hatami, and S. Sarabi, "Enhancing Skin Cancer Diagnosis (SCD) Using Late Discrete Wavelet Transform (DWT) and New Swarm-Based Optimizers," *ArXiv*. Nov. 30, 2024. [Online]. Available: http://arxiv.org/abs/2412.00472

[61] L. I. Mampitiya, N. Rathnayake, and S. De Silva, "Efficient and Low-Cost Skin Cancer Detection System Implementation with a Comparative Study Between Traditional and CNN-Based Models," *J. Comput. Cogn. Eng.*, vol. 2, no. 3, pp. 226–235, Dec. 2022, doi: 10.47852/bonviewJCCE2202482.

[62] E. Farea, R. A. A. Saleh, H. AbuAlkebash, A. A. R. Farea, and M. A. Al-antari, "A hybrid deep learning skin cancer prediction framework," *Eng. Sci. Technol. an Int. J.*, vol. 57, p. 101818, Sep. 2024, doi: 10.1016/j.jestch.2024.101818.

[63] M. S. Ali, M. S. Miah, J. Haque, M. M. Rahman, and M. K. Islam, "An enhanced technique of skin cancer classification using deep convolutional neural network with transfer learning models," *Mach. Learn. with Appl.*, vol. 5, p. 100036, Sep. 2021, doi: 10.1016/j.mlwa.2021.100036.

[64] A. Ameri, "A Deep Learning Approach to Skin Cancer Detection in Dermoscopy Images," *J. Biomed. Phys. Eng.*, vol. 10, no. 6, Dec. 2020, doi: 10.31661/jbpe.v0i0.2004-1107.

[65] Z. Rahman and A. M. Ami, "A Transfer Learning Based Approach for Skin Lesion Classification from Imbalanced Data," in *2020 11th International Conference on Electrical and Computer Engineering (ICECE)*, Dec. 2020, pp. 65–68. doi: 10.1109/ICECE51571.2020.9393155.

[66] K. Lenc and A. Vedaldi, "Understanding image representations by measuring their equivariance and equivalence," in *2015 IEEE Conference on Computer Vision and Pattern Recognition (CVPR)*, Jun. 2015, pp. 991–999. doi: 10.1109/CVPR.2015.7298701.

[67] H. Wang, Q. Qi, W. Sun, X. Li, B. Dong, and C. Yao, "Classification of skin lesions with generative adversarial networks and improved MobileNetV2," *Int. J. Imaging Syst. Technol.*, vol. 33, no. 5, pp. 1561–1576, Sep. 2023, doi: 10.1002/ima.22880.

[68] K. S. Mader, "Skin Cancer MNIST: HAM10000," *Kaggle.com*, 2019. https://www.kaggle.com/datasets/kmader/skin-cancer-mnist-ham10000 (accessed Dec. 06, 2024).